

# The Observed Long- and Short-Term Phase Relation between the Toroidal and Poloidal Magnetic Fields in Cycle 23

S. Zharkov · E. Gavryuseva · V. Zharkova

Received: 16 May 2007 / Accepted: 7 December 2007 / Published online: 6 February 2008  
© Springer Science+Business Media B.V. 2008

**Abstract** The observed phase relations between the weak background solar magnetic (poloidal) field and strong magnetic field associated with sunspots (toroidal field) measured at different latitudes are presented. For measurements of the solar magnetic field (SMF) the low-resolution images obtained from Wilcox Solar Observatory are used and the sunspot magnetic field was taken from the Solar Feature Catalogues utilizing the SOHO/MDI full-disk magnetograms. The quasi-3D latitudinal distributions of sunspot areas and magnetic fields obtained for 30 latitudinal bands (15 in the northern hemisphere and 15 in the southern hemisphere) within fixed longitudinal strips are correlated with those of the background SMF. The sunspot areas in all latitudinal zones (averaged with a sliding one-year filter) reveal a strong positive correlation with the absolute SMF in the same zone appearing first with a zero time lag and repeating with a two- to three-year lag through the whole period of observations. The residuals of the sunspot areas averaged over one year and those over four years are also shown to have a well defined periodic structure visible in every two–three years close to one-quarter cycle with the maxima occurring at  $-40^\circ$  and  $+40^\circ$  and drifts during this period either toward the equator or the poles depending on the latitude of sunspot occurrence. This phase relation between poloidal and toroidal field throughout the whole cycle is discussed in association with both the symmetric and asymmetric components of the background SMF and relevant predictions by the solar dynamo models.

**Keywords** Solar cycle: observations · Sunspots: magnetic fields, statistics

---

S. Zharkov (✉)  
Department of Applied Mathematics, University of Sheffield, Sheffield, UK  
e-mail: s.zharkov@sheffield.ac.uk

E. Gavryuseva  
Arcetri Observatory, University of Florence, Florence, Italy

V. Zharkova  
Department of Computing, University of Bradford, Bradford, UK

## 1. Introduction

Understanding the origin of a magnetic cycle in solar activity is a very important and still unsolved problem in solar physics. The solar cycle is defined by sunspot occurrences, or their areas, which change with a period of 11 or 22 years as observed for more than a few hundred years (Hathaway and Wilson, 2004). The solar cycle is believed to result from a hydromagnetic dynamo that operates from the bottom of the solar convective zone (SCZ) in the solar interior where magnetic flux tubes are formed and travel for about half the cycle time of 11 years to the solar surface to appear as sunspots at the beginning of a new cycle (see reviews by Tobias, 2002; Ossendrijver, 2003; Krivodubskij, 2005). The mechanisms affecting the travel time of the magnetic tubes from the SCZ to the solar surface and their migration in latitude and longitude inside the solar interior define the duration of the solar cycle and the sunspot distribution on the solar surface. Sunspots are also known to migrate in latitude during the solar cycle, with a minority of sunspots migrating toward the poles and the majority migrating toward the equator as shown in Maunder's butterfly diagrams (Maunder, 1904).

At the middle of the previous solar cycle a new poloidal field is assumed to be formed by the dynamo mechanism at the poles. Once this field is brought to the base of the SCZ, it becomes affected by differential rotation of the solar plasma and buoyancy instability, collapsing to form strong toroidal field as magnetic flux tubes. These tubes travel through the solar interior and rise to the surface in the form of  $\Omega$ -shaped loops (Parker, 1955) to form sunspots and active regions. As the cycle progresses, this toroidal field becomes transformed back into a poloidal one by convection and the Coriolis force ( $\alpha$  effect; Krause and Radler, 1980). The more recent dynamo models predict that the latitudinal distributions of the sunspot area and magnetic fields at mid-to-low latitudes where the sunspots emerge (called the "royal zone"; Krivodubskij, 2005) are governed by magnetic-field advection and buoyancy (Kitchatinov and Rudiger, 1999; Dikpati and Gilman, 2001; Nandi and Choudhuri, 2001) allowing magnetic flux tubes to travel upward and appear on the solar surface.

However, despite the many solar dynamo models, there remain many unanswered questions about the dynamo mechanisms. One of them is the phase relation between the poloidal and toroidal fields during the solar cycle. This relation was investigated for oscillatory axisymmetric mean-field dynamo models, which predicted a quadruple symmetry about the equatorial plane and the observed shape of latitudinal distributions in the toroidal magnetic field (Stix, 1976).

The Mt. Wilson Observatory measurements for cycles 20 and 21 have shown that the polarities for sunspot magnetic fields deduced from "butterfly diagrams" were opposite to the polarity of the background solar magnetic field in each hemisphere (Stix, 1976; Vainstein, Zeldovich, and Ruzmaikin, 1980), exhibiting a full-cycle lag between the poloidal and toroidal fields. Then, by restoring the radial magnetic-field components, it was concluded that only models with angular velocity increasing with depth (*i.e.*,  $\frac{\partial\omega}{\partial r} < 0$ ) can reproduce closely enough the shape of the butterfly diagrams (Stix, 1976). This implies that the helicity parameter  $\alpha$  has to be positive to account for meridional flows of dynamo waves, (*i.e.*,  $\alpha \frac{\partial\omega}{\partial r} < 0$ ; Krivodubskij, 2005). However, the positive value of  $\alpha$  contradicts other studies where this parameter is found to change from positive near the surface to negative at the bottom of the SCZ to allow the flux tubes to travel to the surface (Yoshimura, 1981).

Recent observations show that the latitudes where sunspots emerge on the surface in the northern and southern hemisphere vary differently at different phases of the solar cycle. The recent observations of the magnetic tilts of sunspot groups and active region areas and the

total areas covered by sunspots and active regions in the northern and southern hemispheres (counted as a sum of the areas for all the sunspots/active regions detected in a given image) are found to be very asymmetric and to vary periodically during the cycle (Temmer, Veronig, and Hanslmeier, 2002; Zharkova and Zharkov, 2007). Moreover, there is an observed distinct domination of one or another hemisphere with the two basic periods: a long one of 11 years and a shorter one of about 2.5–3 years (or approximately one-quarter cycle) (Zharkov, Zharkova, and Ipson, 2005; Zharkov and Zharkova, 2006).

In addition, strong negative correlation is detected between the average daily latitudinal motions of sunspot groups and their tilt angles: The groups with smaller tilts are normally associated with equatorward drifts (Howard, 1991). Also, toward the maximum of activity the signs of the tilt angle in sunspot groups during their lifetime reverses (Howard, 1991). The groups with tilt angles ( $\theta$ ) near the average show a positive change of daily polarity separation ( $d$ ) between leading and following spots depending on the latitude  $\phi$  as  $\theta/d \approx -0.021\phi - 0.123$  (Holder *et al.*, 2004; Zharkova and Zharkov, 2007).

At the same time, low-resolution observations of the solar magnetic field (SMF) from the Wilcox Solar Observatory (WSO) have shown that the SMF has a well-defined four-zone structure: two polar zones with latitudes above  $\pm 25^\circ$  and two near-equatorial ones for the latitudes ranging from zero to  $\pm 25^\circ$ . The near-equatorial zones have opposite magnetic field polarities in the northern and southern hemispheres that are swapped every two–three years (Gavryuseva, 2006), similar to those detected for sunspots and active regions (Zharkov, Zharkova, and Ipson, 2005; Zharkov and Zharkova, 2006). Therefore, further investigation is required to establish the correlation between the latitude of appearance of magnetic flux tubes, or sunspots, and the variations of the SMF in the opposite hemispheres during different phases of the cycle. This will allow tracking of the relation between the poloidal and toroidal field in cycle 23.

The data for sunspot and active region areas and total fluxes, as well as for the low-resolution solar magnetic field, are described in Section 2. The results of correlation of these two time series at various latitudes and the phase of the solar cycle are discussed in Section 3. Conclusions are drawn in Section 4.

## 2. Data Description and Statistical Tool

### 2.1. Solar Feature Catalogue

The searchable Solar Feature Catalogues (SFCs) with nine-year coverage (1996–2005) are developed from digitized solar images by using automated pattern-recognition techniques (Zharkova *et al.*, 2005). All full-disk images were first automatically standardized in intensity and to a circular shape. Then automated techniques were applied for the detection of sunspots, active regions, filaments, and line-of-sight magnetic neutral lines in full-disk solar images in Ca II K1, Ca II K3, and H $\alpha$  lines taken at the Paris-Meudon Observatory and for the white-light images and magnetograms from SOHO/MDI. The results of the automated recognition were verified with manual synoptic maps and available statistical data, revealing a high detection accuracy of 92–96% (Zharkov, Zharkova, and Ipson, 2005).

Based on the recognized parameters, a relational database of Solar Feature Catalogues was built for every feature and published with various predesigned search pages on the Bradford University Web site (<http://solar.inf.brad.ac.uk/>). At the moment, the catalogue contains 368 676 sunspot features extracted from 10 082 SOHO/MDI continuum observations and around 100 000 active region features starting from 19 May 1996 at 19:08:35 to 31 May

2005. The catalogue is generally accessible via <http://solar.inf.brad.ac.uk> (ASCII and XML files) and through the EGSO-registered Web services and SolarSoft vobs/egso branch.

For detected sunspots the following information is extracted: number of umbrae, Carrington and planar coordinates of the sunspot center of gravity, heliographic area, heliographic diameter, maximum magnetic field, minimum field, excess magnetic flux (EMF), total (absolute) flux, maximum umbra field, minimum umbra field, excess umbra flux, total (absolute) umbra flux, the pixel and planar coordinates of the bounding rectangle, its raster scan marking the penumbral and umbral pixels, and the observational parameters (Zharkov, Zharkova, and Ipson, 2005).

Note that Carrington rotation (CR) number 1910 corresponds to the start of 1996 and CR number 2030 to May 2005. Also note that gaps in the graphs are caused by the absence of MDI data because of technical problems with SOHO in 1998; these periods were excluded from the correlation analysis.

## 2.2. Wilcox Solar Observatory Data

To derive large-scale solar magnetic field variations, we use the low-resolution magnetograms captured daily at the WSO site (<http://wso.stanford.edu/synoptic.html>). The line-of-sight component of the background solar magnetic field (hereafter, solar magnetic field, SMF) is measured from the photosphere by using the Zeeman splitting of the 525.02-nm Fe I spectral line with the WSO's Babcock solar magnetograph. Each longitudinal value is the weighted average of all of the observations made in the longitudinal zone within 55° around the central meridian (Hoeksema, 1985).

The observations of the photospheric magnetic field (SMF) were carried out from the year 1976.405, corresponding to the beginning of the CR 1642, up to the year 2005.16, or CR 2027. The data cover the solar activity cycles 21, 22, and 23 (Scherrer et al., 1977; Hoeksema, 1985). For the purpose of the current study, we consider the averaged magnetic field in cycle 23 only. From this data set we then select a subset within the 30 μ-hemispheres in the heliographic latitude we then select a subset within the 30 μ-hemispheres from 72.5° North to 72.5° South binned in uniform intervals of the sine of the latitude.

## 2.3. Some Elements of Statistics

The correlation analysis can only establish an approximate estimate of the real dependencies between two time series since they do not include many physical influences (e.g., differential rotation, convection, diamagnetic advection, and magnetic buoyancy) that affect the measured data.

Therefore, the compared time series entities might not have a linear dependence and, thus, their correlation coefficients are not expected to be very high. However, their magnitudes above or below zero will indicate the level of relation between them and a time lag, if detected, can suggest a similarity in their periodicities, or phase relation. This statistical analysis is sufficient for understanding the links between the two time series that can provide some input to future models of the solar dynamo.

As is well known, a correlation coefficient indicates the strength and direction of a linear relationship between two random variables, or their departure from being independent. The correlation coefficient  $r$  is defined by the formula

$$r = \frac{\frac{1}{N-1} \sum_{i=0}^{N-1} (x_i - \bar{x})(y_i - \bar{y})}{\sqrt{\frac{1}{N-1} \sum_{i=0}^{N-1} (x_i - \bar{x})^2 \frac{1}{N-1} \sum_{i=0}^{N-1} (y_i - \bar{y})^2}} = \frac{\frac{1}{N} \sum_{i=0}^{N-1} (x_i - \bar{x})(y_i - \bar{y})}{\sigma_x \sigma_y}, \quad (1)$$

where  $N$  is the number of measurements,  $\bar{x}$  and  $\bar{y}$  are the expected values (means) of the series  $X$  and  $Y$ , and  $\sigma_x$  and  $\sigma_y$  are their standard deviations. Depending on the type of correlation we try to obtain, the measurements in both series have to be preprocessed, or averaged, with the averaging filter sliding across the data during the full period of measurements. The filter has a width of a quarter or a half of the period that one tries to detect.

If one is looking for some periodic patterns in the investigated series then a cross-correlation analysis is required to measure a level of similarity of the sunspot characteristics to those of the SMF. This cross-correlation is a function of relative time between the measurements:

$$(X \times Y)(z) = \int X^*(t)Y(z + t) dt, \tag{2}$$

where the integral is taken over the range of the values of  $t$  and the asterisk refers to the complex conjugate.

Another very important characteristic that one needs to check with these series is an autocorrelation, or a measure of how well the measurements match a time-shifted version of itself. The autocorrelation function  $R(t, s)$  is defined as follows:

$$R(t, s) = \frac{E[(X_t - \mu)(X_s - \mu)]}{\sigma^2}, \tag{3}$$

where  $X_t$  and  $X_s$  are the measurements at different times,  $E$  is the expected-value operator, and  $\mu$  is the mean of  $X$ . As a result of the definition, an autocorrelation is always peaked at a zero lag.

According to the dynamo models, one can expect a nonlinear relation between the toroidal and poloidal magnetic fields. Since these are assumed to be associated with the observed sunspot and SMF entities, respectively, one needs to evaluate the residuals of the measured averaged magnitudes and estimate a confidence in their variations. The residual for the  $i$ th measurement of  $X$  is defined as

$$\text{Res}(i) = \frac{\bar{X}_i - \mu}{\frac{S_N}{\sqrt{N}}}, \tag{4}$$

where  $S_N$  is the variance of  $X$ ,  $\bar{X}_i$  is the measured mean of  $X$ , and  $\mu$  is the estimated mean with a four-year averaging filter. This is defined on the basis of the confidence interval calculations relying on Student's  $t$ -distribution which both the measured series (EMF and ESMF) satisfy.

### 3. Results and Discussion

#### 3.1. Latitudinal Distributions of Sunspot and Active Region Areas and Excess Magnetic Flux

##### 3.1.1. Quasi-3D Butterfly Diagrams of the Sunspot Areas and Excess Magnetic Field

Let us investigate latitudinal variations of the total sunspot areas (upper plot) and excess magnetic flux (EMF; bottom plot) presented in Figure 1, which were calculated in narrow latitude strips for the whole longitude range in different Carrington rotations during the whole solar cycle. This plot is similar to the classic Maunder butterfly diagrams for sunspot

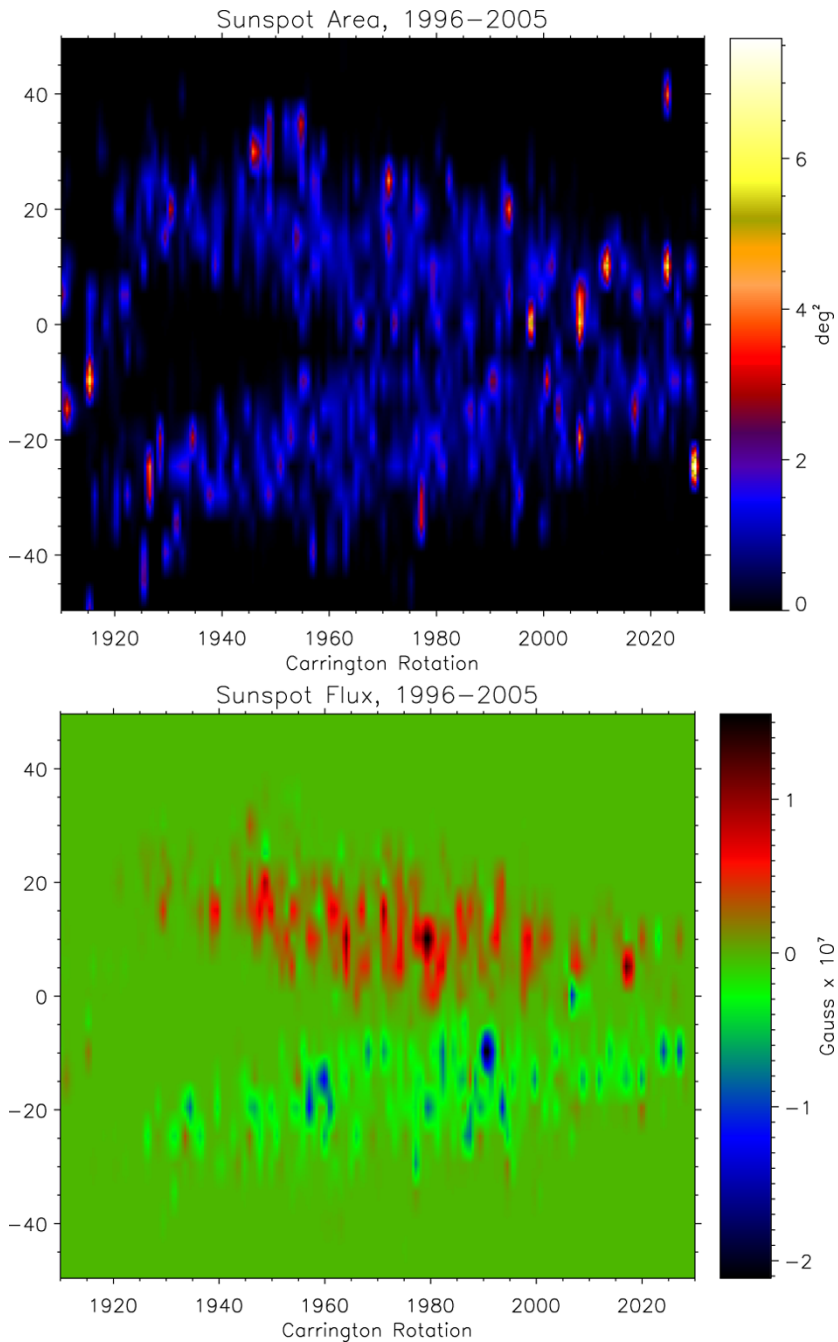


**Figure 1** Butterfly diagrams for cycle 23 for the total sunspot daily areas (upper plot) and excess magnetic fields (lower plot) summed over longitude within two-degree-wide latitudinal strips. The areas are measured in squared degrees and magnetic field in gauss. Note that CR number 1910 corresponds to the start of 1996 and CR number 2030 to May 2005.

appearances (Maunder, 1904) but includes not only the locations of sunspots but also their total area variations in different latitudinal intervals. The total areas of sunspots for a given Carrington rotation are marked with the color scale from a dark black/blue color (corresponding, respectively, to low areas/negative flux) to a yellow white/red (corresponding, respectively, to high areas/positive flux) with the scales presented on the right-hand side of the plot.

Similarly to the previous cycles, the locations of sunspots are confined within the “royal zone” between the latitudes of  $-40^\circ$  and  $+40^\circ$ , as can be seen from Figure 1. At the beginning of the cycle the sunspots emerge at higher latitudes. As the cycle progresses, the sunspot emergence zone slowly moves toward the equator, showing a strong increase in sunspot area during the years of maximum activity.

Additionally, in these two butterfly diagrams one can see fine structure appearing during the activity period as vertical strips in the total areas and magnetic flux. These strips reveal a quasi-periodic mosaic structure changing from one hemisphere to another (*i.e.*, within a given time interval the areas of a particular latitudinal strip in one hemisphere are larger than areas in the symmetric strip in the other hemisphere). Then, for another period, the larger area shifts to another latitude or even to the opposite hemisphere. Let us explore whether a period of these changes can be clearly extracted and, if so, what are the mechanisms causing such quasi-periodic changes.

### 3.1.2. The North–South Asymmetry in the Areas and Excess Magnetic Flux

The total daily areas of sunspots and active regions (AR) and their cumulative areas for northern and southern hemispheres, averaged with the one-year filter, are found to be strongly asymmetric during the whole solar cycle 23 (Figure 2; Zharkov, Zharkova, and Ipson, 2005; Zharkova, Zharkov, and Benkhalil, 2005). This asymmetry is stronger at the beginning of the cycle, approaching the values 0.4 for sunspots and 0.6 for active regions. The North–South asymmetry in the total area variations for both sunspots and ARs also reveals well-defined periodicities with the two basic periods: a longer one covering the whole period of observations (over nine years) and a smaller one of two–three years (close to one-quarter cycle  $\approx 2.75$  years).

There is also a visible asymmetry in the sunspot cumulative areas (Figure 3, upper plot), which is also presented as the asymmetry function (Figure 3, lower plot). Cumulative areas provide additional information about the dynamo mechanism not supplied by the total areas. They can show whether the oscillatory patterns of North–South asymmetries seen in total areas will still be present in cumulative areas and, if so, how long they exist and when they equalize, or whether the dynamo wave decays.

Obviously, at the start of the cycle, when the solar dynamo starts, there are fewer sunspots and the North–South asymmetry is the strongest, as seen in Figure 3. If the solar dynamo does not produce any asymmetry in the interior conditions of both hemispheres affecting the rate of sunspot emergence, as the sunspot number increases we would expect that the symmetry would quickly be restored. However, this is not the case, as one can see in Figure 3.

Similarly to total areas, the cumulative areas at the cycle start in 1996 are dominant in the northern hemisphere, and then, in 2.5–3 years, the southern hemisphere takes over. This pattern repeats again toward the cycle end. Therefore, both periods detected in the total areas are also seen in the cumulative areas. The only difference is that the cumulative areas show the asymmetry decrease, or decay, as  $e^{-kt}$  toward the cycle end, where  $k$  can be determined from Figure 3 as  $k \approx 3.2$ , where  $t$  is the time after the cycle start. This decay can characterize some turbulent processes, which slow down the primary solar dynamo wave to 11 years, and the decay constant  $k$  can be compared with those predicted by solar dynamo models.

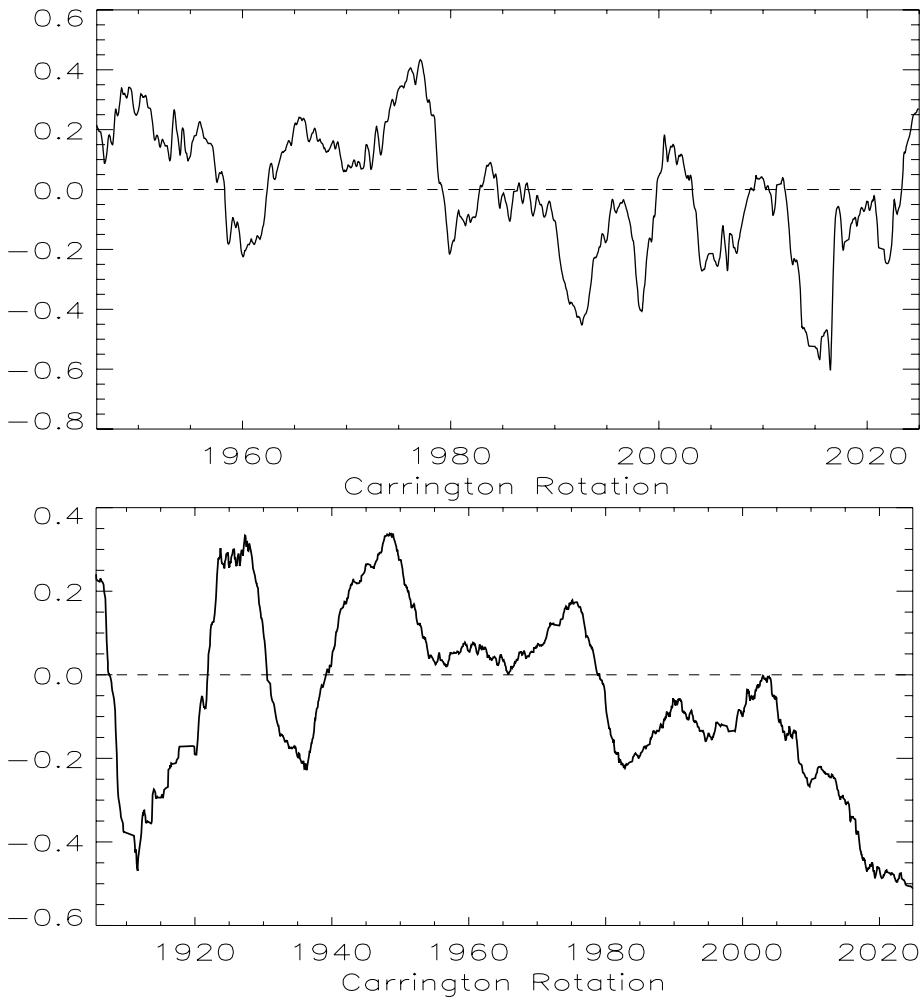


**Figure 2** The North–South area asymmetries in cycle 23 for the total sunspot (upper plot) and active region daily areas (lower plot) averaged over one year.

Even stronger North–South asymmetry is seen in the excess magnetic flux; that is, the magnetic flux added with its sign for the leading and trailing polarities, contained in all sunspots in the northern and southern hemispheres (Figure 4), which reveals a nearly complete polarity separation over the hemispheres similar to those reported for the previous cycles 20 and 21 by Stix (1976). This separation supports the phase delay of about a whole period of 11 years between the poloidal and toroidal fields found by Stix (1976). However, as can be seen the full separation is sometimes violated during the periods coinciding with increased local activity such as the Halloween flares in 2003.

The nature of the larger period was assumed to be related to the dynamo wave governing the whole solar activity suggested by Parker (1955) and refined by many other authors (see the reviews by Tobias, 2002; Ossendrijver, 2003; Krivodubskij, 2005). The nature of the shorter term periodicity still needs to be investigated.



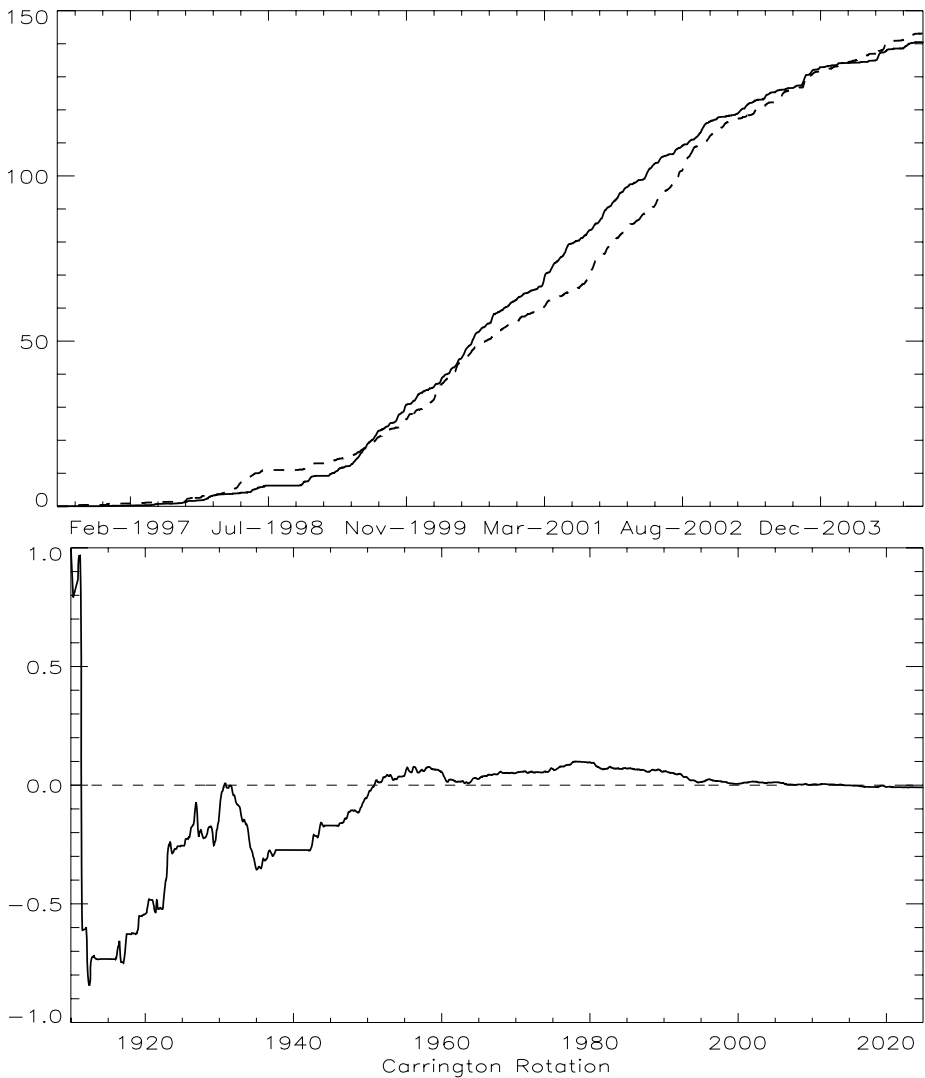


**Figure 3** Upper plot: The cumulative areas in square degrees  $\times 10^3$  for sunspots in northern (solid line) and southern (dashed line) hemispheres. Lower plot: North–South asymmetry in the cumulative areas for the sunspots in cycle 23.

### 3.2. Correlation with the Background Solar Magnetic Field

Because in this study we are interested in periods of the sunspot area and flux variations longer than one year, the measured means ( $\bar{X}_i$ ) can be selected for every measurement by averaging with a one-year filter. Then if someone wishes to define the deviations from the estimated mean within a longer period, say three–four years, then this one-year mean needs to be compared with the four-year estimated mean  $\mu$  (see also Section 2.3). These two approaches to the mean estimations (one and four years) were utilized in the studies presented below.

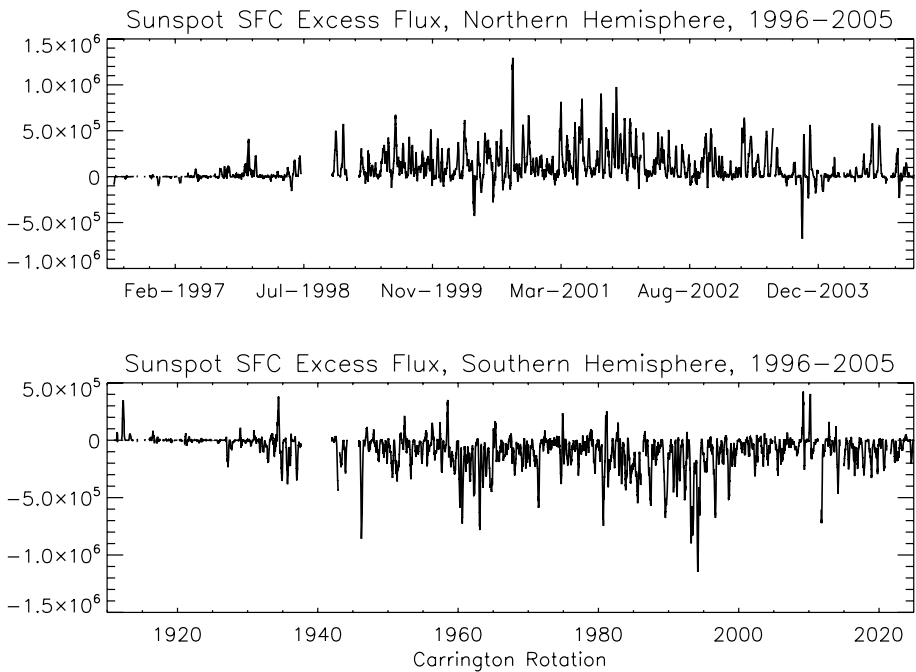


**Figure 4** The line-of-sight excess magnetic flux in sunspots measured separately in the northern and southern hemispheres from the SFC as described by Zharkov and Zharkova (2006).

Because the SMF is assumed to carry the poloidal magnetic field, whereas sunspots or active regions are associated with the toroidal one, then, similarly to the analysis carried out by Stix (1976), a comparison of these time series will allow the relations between these fields for different phases of cycle 23 to be established.

### 3.2.1. Latitudinal Variations of the Background SMF

To understand the distribution of sunspot areas and magnetic fluxes and their dependence on the activity cycle, it is necessary to study the latitudinal distribution of the background SMF. The latter have been deduced and statistically processed (Gavryuseva and Kroussanova, 2003; Gavryuseva, 2006) from the data obtained by the WSO for the past 29 years as described in Section 2.2.

We calculate the SMF averaged over one year and their residuals from the estimated means for four years for the symmetric part [ $SMF(\theta) + SMF(-\theta)$ ; Figure 6, upper plot] and for the asymmetric one [ $SMF(\theta) - SMF(-\theta)$ ; Figure 6, lower plot]. The asymmetric part variations have a period close to 10–11 years for a single polarity exchange or 22 years for the whole polarity exchange. The symmetric SMF component changes its sign every 2.5–3 years, either coinciding with the sign of the leading polarity in a given hemisphere or being opposite to it. As the cycle progresses, both the symmetric and asymmetric components show a constant shift from the equator to the poles with their own phases.

The SMF clearly reveals the four-zonal (4Z) latitudinal structure with the opposite polarity zones with the boundaries located in  $\pm 25^\circ$ ,  $0^\circ$  (two near-equatorial zones and two polar zones), the signs of which also vary with the 22-year period. The polarities of the SMF in

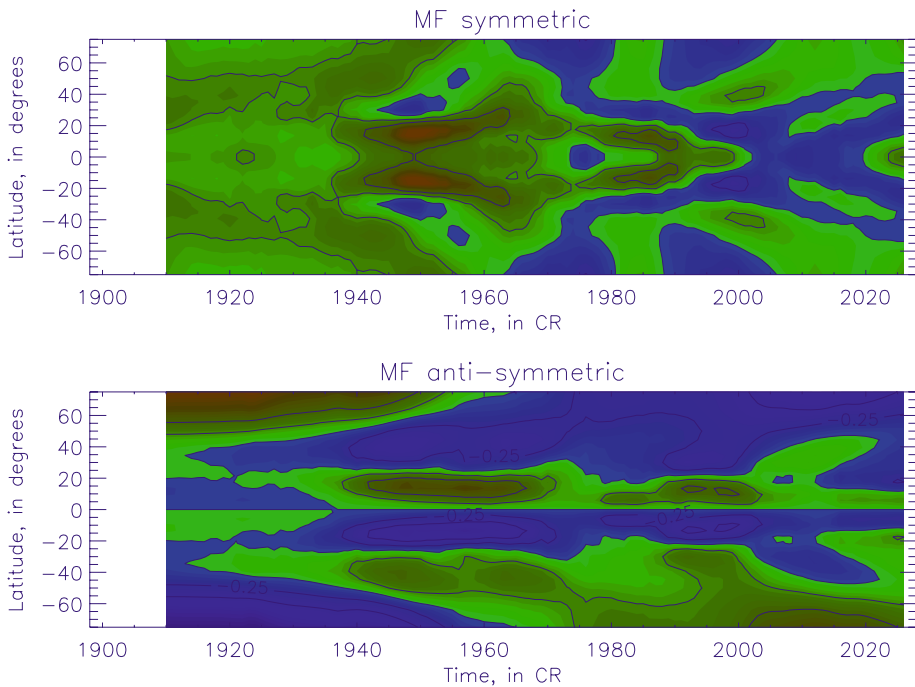


**Figure 5** The one-year-mean SMF for the symmetric component [ $SMF(\theta) + SMF(-\theta)$ ; upper plot] and for the antisymmetric components [ $SMF(\theta) - SMF(-\theta)$ ; lower plot; see Figure 1 and Section 2 for the relation between CR and years]. The green-brown colors correspond to positive polarity and blue-navy to negative polarity; the outer contours correspond to a  $3\sigma$  interval and the inner contours to a  $2\sigma$  interval about the relevant maximum magnetic field (brown or blue).

the near-equatorial zones in both solar hemispheres are opposite and change in the each subsequent cycle (Hathaway, 2005; Gavryuseva, 2006). Also there is a 5.5-year lag between the SMF polarity change in the two near-equatorial and two polar zones (Gavryuseva, 2006). The background magnetic fields in the near-equatorial zones have opposite polarity to the leading parts of most activity regions within. In the polar zone after five–six years after the cycle start, the polarity reverses (Gavryuseva, 2006), coinciding in time with the SMF reversal in the subpolar zones.

A noticeable difference seems to occur between the periods of polarity change in the opposite hemispheres: The longer period appears in the northern hemisphere and shorter one in the southern hemisphere ( $P_{\text{North}} \approx 3$  years and  $P_{\text{South}} \approx 2.5$  years; Gavryuseva, 2006). Because of this difference, the polarity waves in the hemispheres at different moments can be either in phase or antiphase. The magnitude of the mean latitudinal magnetic field in 1996 (at the minimum of the solar activity, CR 1920–1922) was unusual (*i.e.*, positive polarity spreading from the north pole to latitudes of about  $45^\circ - 50^\circ$ ).

### 3.2.2. The Long-Term Phase Relation between the Sunspot Excess Magnetic Flux and the SMF

We compare these SMF variations with those of the sunspot excess magnetic flux averaged over one Carrington rotation (Figure 6). The comparison shows that, similar to cycles 20

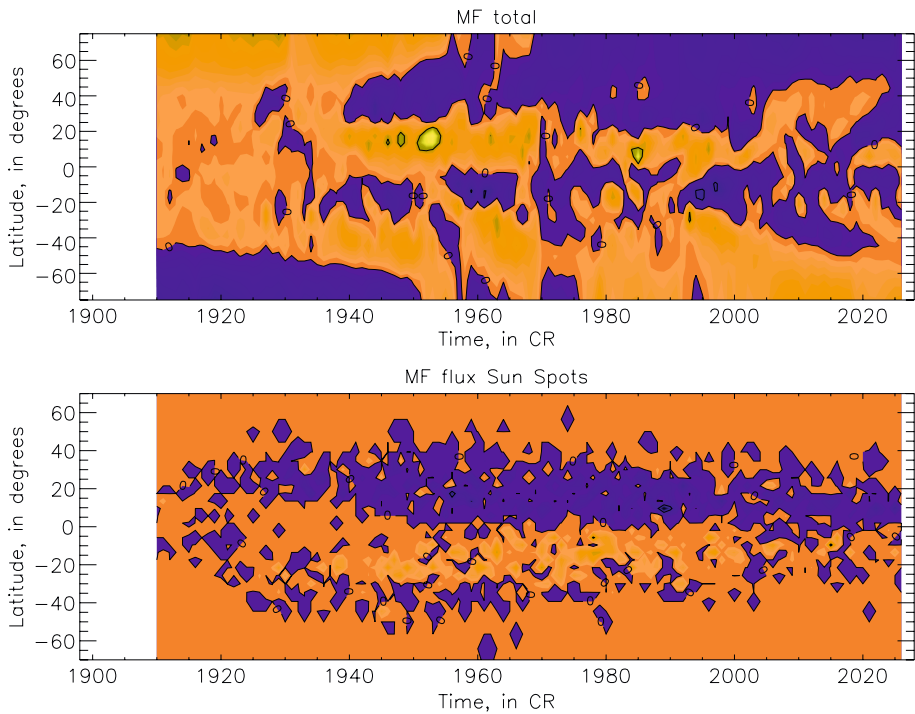


**Figure 6** The latitudinal distributions of the excess solar magnetic field (SMF) (upper plot) and sunspot excess fluxes (bottom plot) in cycle 23 averaged over one Carrington rotation. Blue denotes positive polarity and orange-yellow negative polarity.

and 21 measured by Stix (1976), these fluxes have nearly opposite polarities in the same hemisphere during the whole cycle. This confirms that a large-scale phase relation between the weak poloidal (SMF) and strong toroidal (sunspots) magnetic field is close to a whole cycle period ( $\approx 11$  years) found by Stix (1976). However, this polarity parity is not fully fulfilled in equatorial zones or, especially, in the polar zones.

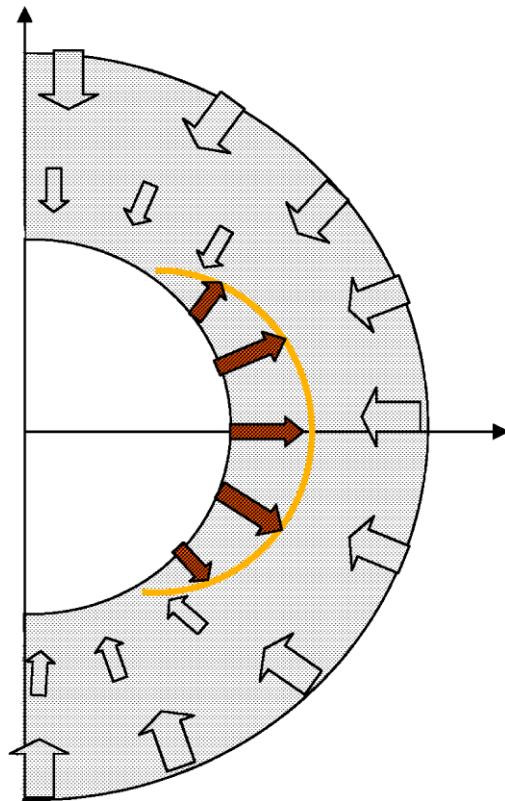
These variations fit the axisymmetric dynamo models rather well, with the phase of a full cycle period between the poloidal and toroidal fields (see Figures 6 and 7 in Stix, 1976) and with the upward magnetic advection in “the royal zone” (the orange line in Figure 7) supporting the upward buoyancy of flux tubes from the solar convective zone and their appearance on the solar surface as sunspots and active regions (Rudiger and Brandenburg, 1995; Kitchatinov and Rudiger, 1999; Belvedere, Kuzanyan, and Sokoloff, 2000; Krivodubskij, 2005).

### 3.2.3. The Short-Term Phase Relation between the SMF and the Sunspot EMF

To understand the nature of short-term oscillations in sunspot characteristics, let us rebuild the quasi-butterfly diagrams of the daily EMF and SMF variations with one-year and four-year filters (see also Section 2.3). Then by calculating the residuals of the sunspot areas, one-year minus four-year, one can reveal periodicities within a scale of less than three years (see Figure 8).

The residuals of the sunspot areas, similar to those in the SMF, vary quasi-periodically, revealing either much lower (blue colors) or much higher (green and brown colors) areas

**Figure 7** Meridional cross section of the solar convective zone with the distributions of radial velocity of the toroidal field advection in depth and latitude (with the equator marked by the horizontal axis). The arrows denote the advection directions: black – downward pumping suppressing the magnetic buoyancy; brown – upward pumping supporting the magnetic buoyancy within the “royal zone” (orange line). (Courtesy of Krivodubskij.)



than the areas averaged over four years. Each pattern lasts for 2.5–3 years over the whole period of the observations, with its sign reversing in the next 2.5- to 3-year period. This indicates that such a periodicity in both EMF and the SMF could be related. Let us establish the phase of such a relation.

To check how stable the period of short-term oscillations is (two–three years, or 1/4 cycle) let us cross-correlate the latitudinal distributions in the northern and southern hemispheres for sunspot areas of the EMF and the SMF averaged over one year; the results are shown in Figure 9. As expected, the correlation of sunspot areas in both hemispheres is positive for a time lag of less than three years (Figure 9, upper plot) and becomes negative for larger time lags, whereas the North–South correlation of the sunspot EMF (Figure 9, middle plot) is negative for the first 2.5–3 years and becomes positive in the next three years.

The additional feature appearing for the excess SMF (Figure 9, bottom plot) is the polarity of each periodic structure being opposite in each hemisphere and changing signs in 2.5–3 years, like changing colors on a chess board. Basically, in Carrington rotations 1930–1940 (years 1996–1997) the polarity is negative in the northern hemisphere and positive in the southern one; after 2.5–3 years, the situation is opposite. Then this pattern with changing polarities repeats every 2.5–3 years. Obviously, in some of these periods the polarity of the SMF will be opposite to the leading polarity of sunspots whereas in others it will coincide with it.

Let us correlate each of these two series related to sunspots (areas and EMF) directly with the background SMF (see Figure 10). The variations of the total sunspot areas in cycle 23

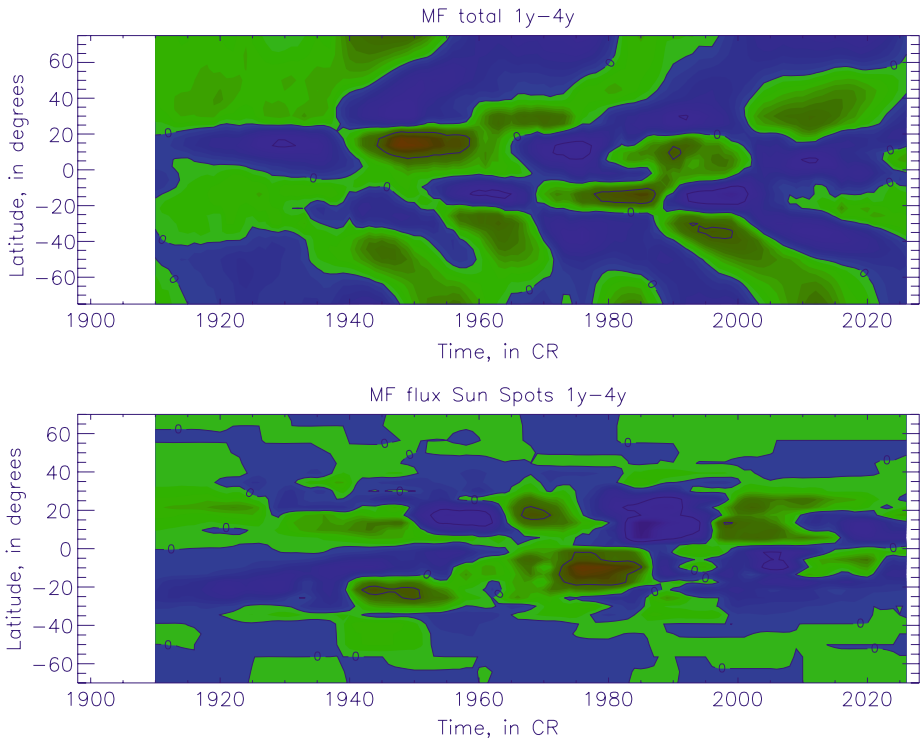


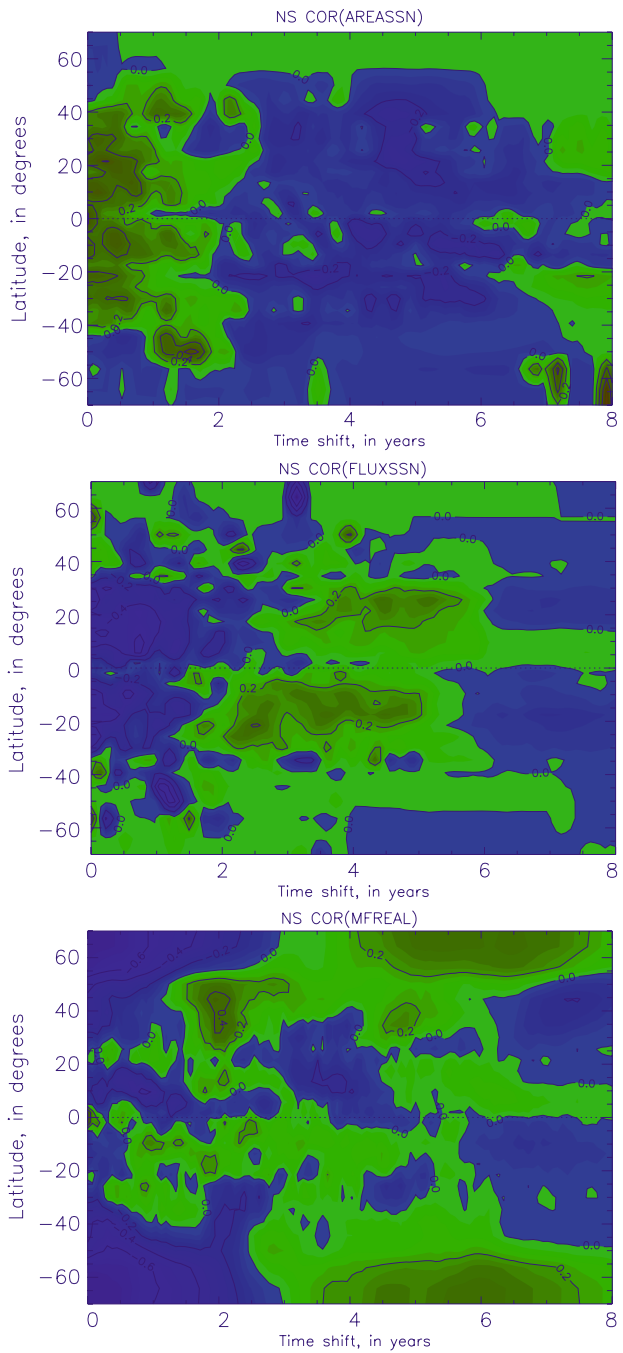
**Figure 8** The residuals in the latitudinal distributions in cycle 23 averaged over one year minus those over four years for excess SMF (upper plot) and excess sunspot flux (bottom plot). The green-brown color presents the positive residuals and the blue one denotes the negative ones (see Figure 1 and Section 2 for the relation between CR and years); the residuals for inner contours are twice as high as those for outer ones.

averaged over one year with one CR step (upper plot) and their residuals from the areas averaged over four years (bottom plot) were correlated with the SMF data for different time lags. The one-year-averaged areas show a strong positive correlation with the background SMFs around zero time lag and a strong negative one at about 50 Carrington rotations (about three years, or 1/4 cycle). The time lag increases from the polar zone in the southern hemisphere through the equator to the polar zone in the northern one.

The residuals for the 1 y–4 y sunspot areas and the SMF (Figure 10, bottom plot) reveal that, similarly to SMF variations, the correlation also has a four-zone structure: The time lag increases in the two zones in each hemispheres, from the top of the royal zones toward either the equator or the poles. The former corresponds to the SMF shift and the migration of sunspot locations shown in the butterfly diagrams in Section 3.1.1; the latter corresponds to the SMF migration toward the poles shown in Section 3.2.1. This correlation changes its sign every 2.5–3 years, similarly to the symmetric variations of the background SMF presented in Figure 5 in Section 3.2.1.

Moreover, correlation of the one-year minus four-year sunspot EMF distribution with the excess SMF one (the bottom plot in Figure 11) also splits into four zones, similar to the four zones of the background SMF reported in Section 3.2.1. In the southern near-equatorial zone there is a positive correlation that increases in time toward the equatorial latitudes with a time lag up to  $\approx$  three years and in the northern near-equatorial zone there is a negative correlation that increases toward the equator with a similar time lag. Then in the next three

**Figure 9** Phase relation between the SMF and sunspot areas (upper plot), excess magnetic flux (middle plot), and the excess SMF (lower plot) in the northern and southern hemispheres for the time lags in years. Numbers labeling the contours show the correlation coefficients.



years the signs of the correlation change in each near-equatorial zone to the opposite one. In the zones from the poles toward the top of the “royal zones” in each hemisphere at the

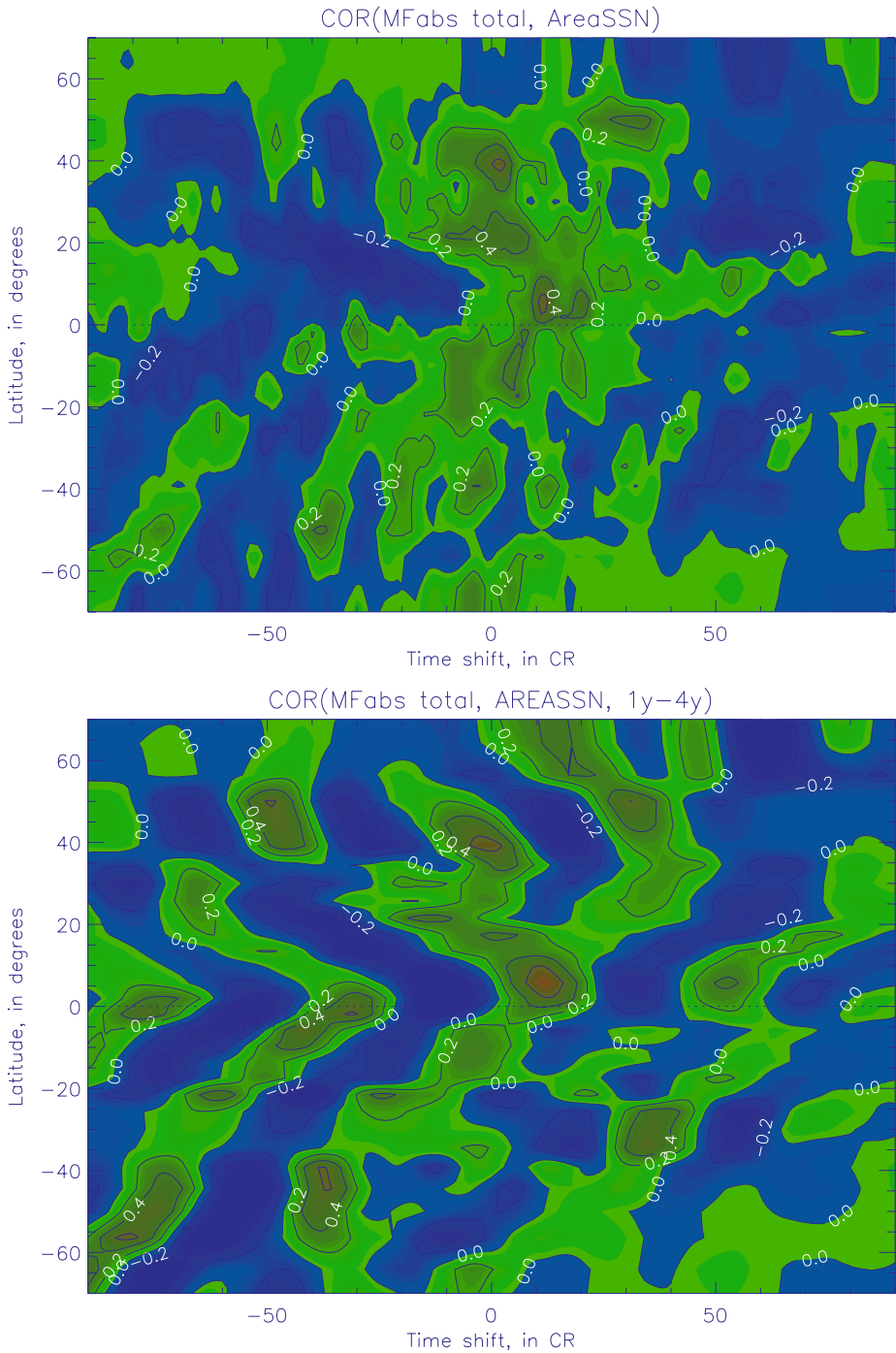


**Figure 10** Correlation between sunspot areas and the SMF averaged over one year with one CR step (top plot) and their residuals from those averaged over four years (bottom plot). The green and brown (blue) colors indicate positive (negative) correlation; the numbers labeling the contours denote the correlation coefficients (0.6, 0.4, and 0.2 from inner to outer contours, respectively).



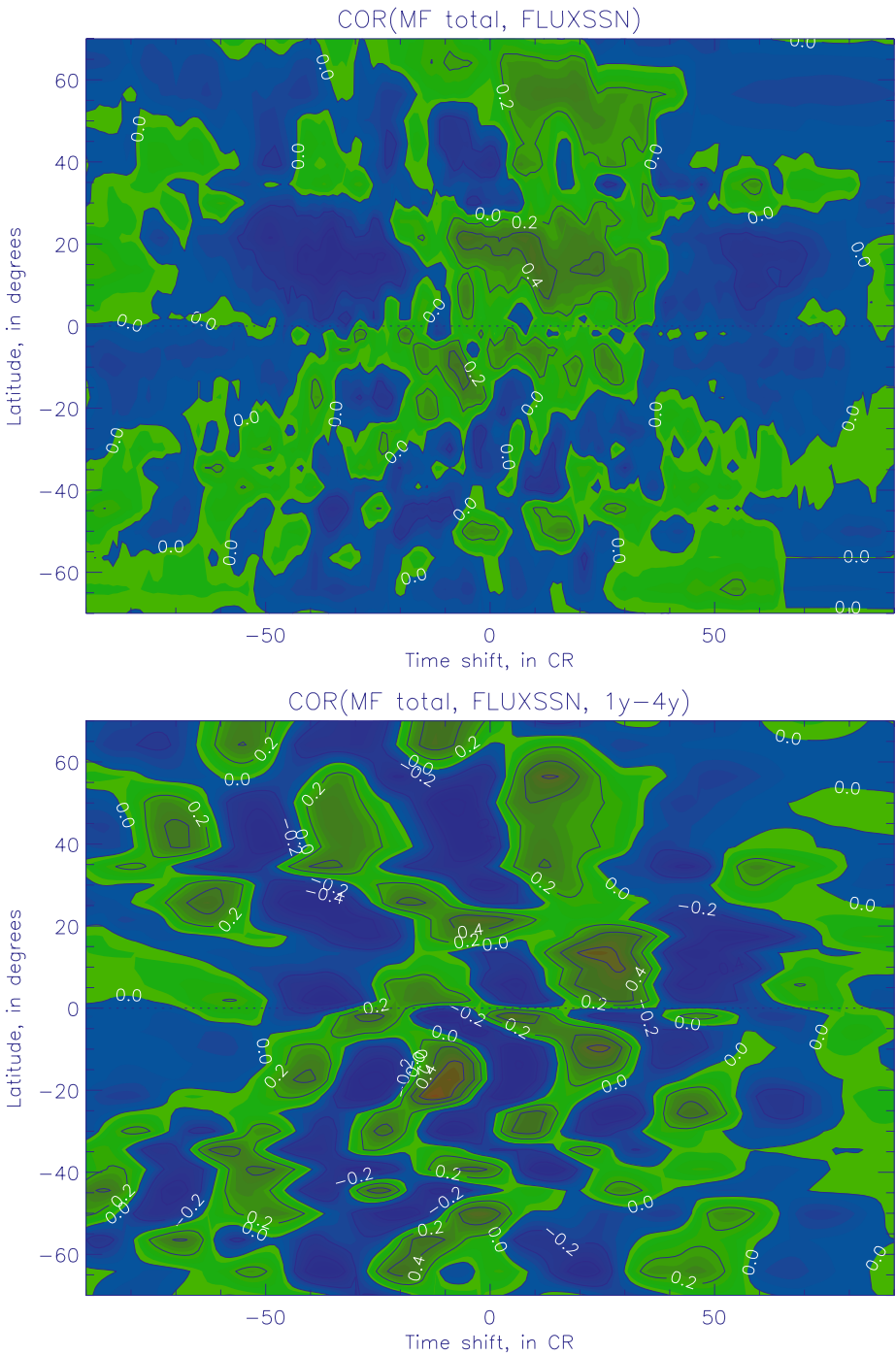


**Figure 11** Correlation between sunspot excess magnetic field and the SMF averaged over one year with one CR step (top plot) and their residuals from those averaged over four years (bottom plot). The green and brown (blue) colors indicate positive (negative) correlation; the numbers labeling the contours denote the correlation coefficients (0.6, 0.4, and 0.2).

beginning of the cycle a negative correlation is established with a four- to five-year lag, changing to the positive one lasting for next five–six years of the cycle.

This correlation together with the correlation of the absolute magnetic flux (magnetic field strength confined in sunspots) with sunspot areas and EMF (top and bottom plots in Figure 11, respectively) lends support to the suggestion that, in addition to a long phase relation of about a whole cycle (11 years) between the poloidal and toroidal fields, there is also a shorter phase of about  $1/4$  cycle  $\approx 2.75$  years when the signs of the SMF polarity in each hemisphere are changed. These changes seem to modulate the borders of the “royal zone” where magnetic pumping allows flux tubes to float to the solar surface (the red line in Figure 7). This, in turn, leads to the asymmetric fluctuations of the symmetric component of the poloidal field in the northern and the southern hemispheres (see Figure 6 in Stix, 1976). If the sign of the SMF in this period coincides with the leading polarity sign, the SMF suppresses flux-tube buoyancy and the frequency of sunspot appearances; if this sign is opposite to the leading polarity, it increases sunspot appearances; and when it coincides with the leading polarity, it suppresses them.

#### 4. Conclusions

We have established a correlation between the appearances of magnetic flux tubes as sunspots at different latitudes of each hemisphere and the latitudinal variations of solar magnetic field during different phases of solar cycle 23.

We have found that there are four zones in the SMF distributions, leading to four similar zones in sunspot areas and EMF distributions: two near-equatorial zones located between the latitudes of  $-40^\circ$  and  $+40^\circ$ , called the “royal zone” (Figure 7), and two polar zones located above these latitudes. Similarly to the previous cycles, the locations of sunspots are confined within the “royal zone,” as expected from a magnetic pumping effect producing the upward velocities of toroidal field advection (Krivodubskij, 2005). At the beginning of the cycle the formation of sunspots is located at higher latitudes; as the cycle progresses the formation zone slowly moves toward the equator. In both subpolar zones the sunspots and their EMF move toward the poles.

Additionally, in the butterfly diagrams for sunspot areas and EMF built in the “royal zone”, one can see a striplike fine structure in latitude appearing during the activity period as vertical threads. This feature points to a strong increase in the solar surface areas covered by sunspots at some latitudes in one hemisphere or another. Then over the subsequent time interval the sunspot area/EMF increase shifts to the opposite hemisphere, revealing a repeating striplike, or a quasi-periodic, temporal structure.

A period of about 2.5–3.0 years can be extracted from these strip appearances in sunspot areas and excess magnetic flux if the values are averaged over one year and their residuals are defined from those averaged over four years. These periods are also confirmed by strong positive correlation with the symmetric part of the background solar magnetic field, which itself reveals a well-defined four-zonal latitudinal structure in each hemisphere with the boundaries located along the tops of the “royal zones.” Since the SMF is assumed to carry the poloidal magnetic field whereas sunspots or active regions are associated with the toroidal magnetic field, then, similar to the analysis carried out by Stix (1976), a comparison of these time series allowed us to establish the relations between them for different phases of cycle 23.

The overall magnetic polarities of EMF and SMF in opposite hemispheres averaged over one Carrington rotation are opposite throughout the whole cycle. Although their magnetic

polarities averaged by one year in the symmetric latitudinal zones of the northern and southern hemispheres are also opposite, they change their signs periodically every 2.5–3 years, either coinciding with the leading polarity in a given hemisphere or being opposite to it. The correlation between the SMF and EMF is either negative when the SMF coincides with the leading magnetic polarity and suppresses the magnetic flux tube buoyancy to the surface or positive when the SMF is opposite to the leading polarity, thus reducing the total magnetic field and supporting the flux tube appearance on the surface.

This, in turn, leads to a period of 2.5–3 years when in one hemisphere its SMF favors sunspot formation, resulting in higher sunspot areas and EMF averaged by one year than in the other hemisphere; then the polarities swap and the sunspot areas and EMF in the other hemisphere become higher. Therefore, the magnetic field confined in the sunspot EMF and background SMF reveals two periods of their phase relation: a long-term one of 11 years, similar to those reported by Stix (1976), and a short-term period of about 2.5–3 years (or close to one-quarter cycle) established in this paper.

These modulations of sunspot characteristics by the SMF can explain the persistent periodic North–South asymmetries in sunspot areas and excess magnetic flux detected from the SFCs for cycle 23. Evidently, to determine the dynamo mechanisms capable of accounting for the short-term ( $\approx$  one-quarter cycle) oscillations in the SMF that lead to the observed variations of sunspot areas and EMF reported in the present study, the qualitative explanation of the periodicity presented in this paper requires the support of theoretical simulations with nonaxisymmetric solar dynamo models. This topic will be discussed in a future paper.

**Acknowledgements** The authors thank the referee for the constructive comments from which the paper strongly benefited. E.G. thanks the University of Bradford for hospitality and inspiration during her visit when the paper was initiated. S.Z. acknowledges the funding from STFC, UK, that partially supported this research.

## References

- Belvedere, G., Kuzanyan, K.M., Sokoloff, D.: 2000, *Mon. Not. Roy. Astron. Soc.* **315**, 778.
- Dikpati, M., Gilman, P.A.: 2001, *Astrophys. J.* **559**, 428.
- Gavryuseva, E.: 2006, *News Acad. Sci. Izv. RAN Ser. Phys.* **70**(1), 102.
- Gavryuseva, E., Kroussanova, N.: 2003, In: *Proc. of the 10th International Solar Wind Conference, Conf. Proc.* **679**, Am. Inst. Phys., Melville, 242.
- Hathaway, D.H.: 2005, In: Sankarasubramanian, K., Penn, M., Pevtsov, A. (eds.) *How Large-Scale Flows May Influence Solar Activity? Conference Series* **346**, Astron. Soc. Pac., San Francisco, 19.
- Hathaway, D.H., Wilson, R.M.: 2004, *Solar Phys.* **224**, 5.
- Hoeksema, J.T.: 1985, <http://sun.stanford.edu>.
- Holder, Z., Canfield, R.C., McMullen, R.A., Nandy, D., Howard, A.F., Pevtsov, A.A.: 2004, *Astrophys. J.* **611**, 1149.
- Howard, R.F.: 1991, *Solar Phys.* **136**, 251.
- Kitchatinov, L.L., Rudiger, G.: 1999, *Astron. Astrophys.* **344**, 911.
- Krause, F., Radler, K.H.: 1980, *Mean Field Magnetohydrodynamics and Dynamo Theory*, Academic, Berlin.
- Krivodubskij, V.N.: 2005, *Astron. Nachr.* **326**, 61.
- Maunder, E.W.: 1904, *Mon. Not. Roy. Astron. Soc.* **64**, 747.
- Nandi, N., Choudhuri, A.R.: 2001, *Astrophys. J.* **551**, 576.
- Ossendrijver, M.: 2003, *Astron. Astrophys. Rev.* **11**, 287.
- Parker, E.N.: 1955, *Astrophys. J.* **121**, 491.
- Rudiger, G., Brandenburg, A.: 1995, *Astron. Astrophys.* **296**, 557.
- Scherrer, P.H., Wilcox, J.M., Svalgaard, L., Duvall, T.L., Dittmer, Ph.H., Gustafson, E.K.: 1977, *Solar Phys.* **54**, 353.
- Stix, M.: 1976, *Mon. Not. Roy. Astron. Soc.* **47**, 243.
- Temmer, M., Veronig, A., Hanslmeier, A.: 2002, *Astron. Astrophys.* **309**, 707.
- Tobias, S.M.: 2002, *Phil. Trans. Roy. Soc. Lond.* **360**, 2741.

- Vainstein, S.I., Zeldovich, Ya.B., Ruzmaikin, A.A.: 1980, *Turbulent Dynamo in Astrophysics*, Nauka, Moscow.
- Yoshimura, H.: 1981, *Astrophys. J.* **247**, 1102.
- Zharkov, S.I., Zharkova, V.V.: 2006, *Adv. Space Res.* **38**(N5), 868.
- Zharkov, S.I., Zharkova, V.V., Ipson, S.S.: 2005, *Solar Phys.* **228**, 401.
- Zharkova, V.V., Zharkov, S.I.: 2007, *Adv. Space Res.* doi:[10.1016/j.asr.2007.02.082](https://doi.org/10.1016/j.asr.2007.02.082).
- Zharkova, V.V., Zharkov, S.I., Benkhalil, A.K.: 2005, *Mem. Soc. Astron. Ital.* **75**, 1072.
- Zharkova, V.V., Ipson, S.S., Zharkov, S.I., Benkhalil, A., Abouadarham, J., Fuller, N.: 2005, *Solar Phys.* **228**, 134.